



UNIVERSITÀ  
DEGLI STUDI  
FIRENZE

SCUOLA DI INGEGNERIA

CORSO DI LAUREA IN INGEGNERIA INFORMATICA

---

# IMAGE SPLICING DETECTION WITH LOCAL ILLUMINANT ESTIMATION

*Candidato*

Lorenzo Cioni

*Relatori*

Prof. Alessandro Piva

Prof. Carlo Colombo

*Correlatori*

Dott. Massimo Iuliani

Dott. Marco Fanfani

---

ANNO ACCADEMICO 2015/2016

*Dedica*

# Contents

<b>Contents</b>	<b>ii</b>
<b>Introduction</b>	<b>1</b>
<b>1 Related work</b>	<b>4</b>
1.1 Image forgery . . . . .	4
1.2 Image forgery detection techniques . . . . .	5
1.3 Image splicing . . . . .	5
1.3.1 Some famous cases . . . . .	6
1.4 Methods based on light inconsistencies . . . . .	8
1.4.1 Inconsistencies in the light setting . . . . .	9
1.4.2 Inconsistencies in the shadows . . . . .	9
1.4.3 Inconsistencies in light color . . . . .	10
1.5 Illuminant color estimation . . . . .	12
1.5.1 Illuminant maps . . . . .	14
1.5.1.1 Generalized Greyworld estimation . . . . .	14
1.5.1.2 Inverse Intensity-Chromaticity estimation . . . . .	15
1.6 Human faces splicing detection . . . . .	18
1.6.1 Method drawbacks . . . . .	19
1.7 Region splicing detection . . . . .	20
1.7.1 Method drawbacks . . . . .	22
<b>2 Proposed approach</b>	<b>23</b>
2.1 Overview . . . . .	23
2.2 Face splicing detection module . . . . .	24

---

2.3	Region splicing detection module . . . . .	24
2.3.1	Image segmentation . . . . .	25
2.3.2	Band illuminant estimation . . . . .	26
2.3.3	Reference illuminant estimation . . . . .	26
2.3.4	Feature vector estimation . . . . .	26
2.3.5	Band classification . . . . .	26
2.3.6	Detection map . . . . .	26
<b>3</b>	<b>Experiments and results</b>	<b>27</b>
3.1	Evaluation datasets . . . . .	27
3.1.1	Colorchecker . . . . .	27
3.1.2	DSO-1 . . . . .	28
3.1.3	DSI-1 . . . . .	28
3.1.4	NIMBLE . . . . .	29
3.2	Test cases . . . . .	29
3.3	Performance . . . . .	29
	<b>Conclusions</b>	<b>30</b>
	<b>Bibliography</b>	<b>31</b>
	<b>Ringraziamenti</b>	<b>33</b>

# Introduction

Recently advanced image processing tools and computer graphics techniques make it straightforward to edit or modify digital images. In a forensics scenario, this raises the challenge of discriminating original images from malicious forgeries. Particular region from an image is pasted into other image with purpose to create image splicing.

Image splicing is a common type of image tampering (manipulation) operation. The image integrity verification as well as identifying the areas of tampering on images without need to any expert support or manual process or prior knowledge original image contents is now days becoming the challenging research problem.

Investigating image's lighting is one of the most common approaches for splicing detection. This approach is particularly robust since it's really hard to preserve the consistency of the lighting environment while creating an image composite (i.e. a splicing forgery).

In this scenario, there are mainly two main approaches:

1. based on the object-light geometric arrangement
2. based on illuminant colors

We focused our attention on the illuminant-based approach, which assumes that a scene is lit by the same light source. More light sources are admitted but far enough such as to produce a constant brightness across the image. In this condition, pristine images will show a coherent illuminant representation; on the other hand, inconsistencies among illuminant maps will be exploited for splicing detection.

*Illuminant Maps* locally describes the lighting in a small region of the image. In the computer vision literature exists many different approaches for determining the illuminant of an image has been proposed. In particular, such techniques are divided into two main groups: statistical-based and physics-based approaches.

Regarding the first group, we start investigating on the *Grey-World algorithm* [1], which is based on the Grey-World assumption, i.e. the average reflectance in a scene is achromatic. In [6], this algorithm proved to be special instances of the Minkowski-norm. Van de Weijer et al. [16] than proposed an extension of the Gray-World assumption, called *Gray-Edge hypothesis* [16], which assumes that the average of the reflectance differences in a scene is achromatic. The reflectance differences can be determined by taking derivatives of the image. Therefore, the authors present a framework with which many different algorithms can be constructed. We focus our attention on the last case, called generalized *Grey-World algorithm (GGE)*. The resulting illuminant maps presents also global illuminant features because of the gray-world and grey-edge assumptions.

For the latter group, was investigate the method proposed by Riess et al. [12], which extends the *Inverse Intense Chromaticity (IIC)* space approach proposed by Tan et al. [14] and tries to model the illuminants considering the dichromatic reflection model [15]. In this case, the illuminant map is evaluated dividing images into blocks, named superpixels, of approximately the same object color, then the illuminant color is evaluated for each block solving the lighting models locally.

Carvalho et al. [2] then presents a method that relies on a combination of the two approaches for the detection of manipulations on images containing human faces. In addition to maps, a large set of shape and texture descriptors are used together. Note that, from a theoretical viewpoint, it is advantageous to consider only image regions that consist of approximately the same underlying material:

for this reason, in [2] the authors focused their analysis on human faces.

In [2] it is also shown that the difference between the two maps, GGE and IIC, increased when fake images are processed. This insight leads to the idea that it is possible to localize tampered image regions simply by considering IM differences with some metric, avoiding the computation of multiple descriptors.

# Chapter 1

## Related work

### 1.1 Image forgery

When dealing with a digital image, it is quite common to wonder if it is original or has been counterfeited in some way. Images and videos have become the main information carriers in the digital era and used to store real world events, but they are very easy to manipulate because of the availability of the powerful editing software and sophisticated digital cameras.

The contexts where doctored pictures could be involved are very disparate; they could be used in a tabloid or in an advertising poster or included in a journalistic report but also in a court of law where digital (sometimes printed) images are presented as crucial evidences for a trial in order to influence the final judgement. So, especially in the last case, reliably assessing image integrity becomes of fundamental importance [19] [4].

*Image forensics* specifically deals with such issues by studying and developing technological tools which generally permit determining, by only analyzing a digital photograph (i.e., its pixels), if that asset has been manipulated or even which could have been the adopted acquisition device (such an issue is not relevant to the topic of the present paper) [5]. Moreover, if it has been established that something has been altered, it could be important to understand in which part of the image itself such a modification occurred, for instance, if a person or a specific object has been covered, if an area of the image has been cloned,



if something (i.e., a face or a weapon) has been copied from another different image, or, even more, if a mixture of these processes has been carried out.

## 1.2 Image forgery detection techniques

To verify the authenticity of a picture many techniques have been identified that can be categorized into active (intrusive) and blind (non-intrusive).

Operative techniques involve a phase of preprocessing the image itself at the time of its creation in order to include some additional information that will be used during the analysis phase. An example of operative technique is the watermarking.

Passive techniques analyze the content of the image using various statistics or semantic content in order to identify inconsistencies of some kind. This approach does not alter the contents of the image. There is a general technique, suitable to capture all kinds of inconsistencies present in an image, but each different method specialises in the identification of a particular type.

## 1.3 Image splicing

Image splicing is a very common type of infringement which basically consists in copying a region of a given image to another, thus creating a composition of two different pictures together.

Image splicing consists of using parts of two or more images to compose a new image that never took place in space and time.

This composition process includes all the necessary operations (such as brightness and contrast adjustment, affine transformations, color changes, etc.) to construct realist images able to deceive viewer. In this process, normally, we refer to the parts coming from other images as aliens and the image receiving the other parts as host.

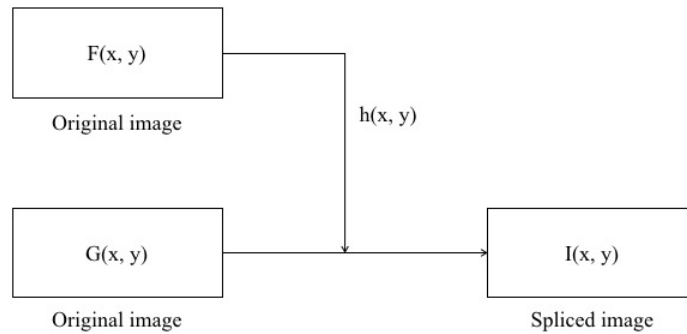


Figure 1.1: Image splicing process

One of the common studied case is image composition involving people are very popular and are employed with very different objectives.

### 1.3.1 *Some famous cases*

Photography has lost its innocence since the early days of his birth. In fact already in 1860, only a few decades after Niépce created the first photo, the first manipulated photographs were identified in 1826. With the advent of digital cameras, camcorders and sophisticated photo editing software, digital image manipulation is becoming more common.

**O.J. Simpson - June 1994** This altered photography O.J. Simpson appeared on the cover of the magazine Time Magazine, soon after his arrest for murder.

In fact, the photograph was altered compared to the original image that has appeared on the cover of Newsweek magazine. Time magazine was accused of manipulation of the photography in order to make darker and menacing figure of Simpson.



Figure 1.2: The Time Magazine and O.J. Simpson

**Iraq - April 2003** This composition of a British soldier in Basra, which keeps pointing toward a civilian Iraqi gesticulates covered, she appeared on the cover of the Los Angeles Times, immediately after the invasion of Iraq.



Figure 1.3: An example of image composition

Brian Walski, a staff photographer for the Los Angeles Times and a veteran of the news with thirty years of experience, was summarily fired from his publisher for their merged two of his shots in order to improve the composition.

### George W. Bush - March 2004

This image, taken from promo released for the election campaign of George w. Bush, outlined a packed audience of soldiers as a backdrop to a child who was flying the American flag. This image was digitally souped-up, using a crude copy and paste, removing Bush from the podium.

After admitting the tampering with the staff of the television station edited and sent to Bush promo with the original photo.

Cases such as this show how present image composition is in our daily lives. Unfortunately, it also decreases our trust on images and highlights the need for developing methods for recovering back such confidence.



Figure 1.4: An example of image composition

## 1.4 Methods based on light inconsistencies

Methods for detecting image composition have become actual and powerful tools in the forensic analysis process. Different types of methods have been proposed for detecting image composition. Methods based on inconsistencies in compatibility metrics, JPEG compression features and perspective constraints are just a few examples of inconsistencies explored to detect forgeries.

After studying and analyzing the advantages and drawbacks of different types of methods for detecting image composition, this work herein relies on the research hypothesis that image illumination inconsistencies are strong and powerful evidence of image composition.

This hypothesis has already been used by some researchers in the literature whose work will be detailed in the next chapter, and it is specially useful for detecting image composition because, even for expert counterfeiters, a perfect illumination match is extremely hard to achieve. Also, there are some experiments that show how difficult is for humans perceive image illumination inconsistencies.

We can divide methods that explore illumination inconsistencies into three main groups of methods:

1. methods based on inconsistencies in the **light setting**: this group of methods encloses approaches that look for inconsistencies in the light position and in models that aim at reconstructing the scene illumination conditions.
2. methods based on inconsistencies in the **shadows**: this group of methods encloses approaches that look for inconsistencies in the scene illumination using telltales derived from shadows.
3. methods based on inconsistencies in **light color**: this group of methods encloses approaches that look for inconsistencies in the color of illuminants present in the scene.

### 1.4.1 *Inconsistencies in the light setting*

Johnson and Farid [10] proposed an approach based on illumination inconsistencies, looking for chromaticity aberrations as an indicator of image forgery. They analyzed the light source direction from different objects in the same image trying to detect traces of tampering. The authors start by imposing different constraints for the problem:

1. All the analyzed objects have *Lambertian surface*<sup>1</sup> [11].
2. The surface reflectance is constant.
3. The object surface is illuminated by an infinitely distant light source.

Using RGB images, the authors assume that the chromaticity deviation is constant (and dependent on each channel wavelength) for all color channels and create a model, based on image statistical properties, of how the ray light should split for each color channel. Given this premise and using the green channel as reference, the authors estimate deviations between the red and green channels and between the blue and green channels for selected parts of the image. Inconsistencies on this split pattern are used as telltales to detect forgeries.

A drawback of this method is that chromaticity deviation depends on the camera lens used to take the picture.

### 1.4.2 *Inconsistencies in the shadows*

Another set of methods is based on inconsistencies on the shadows in the image.

Zhang and Wang [18] proposed an approach that utilizes the planar homology [13], which models the relationship of shadows in an image for discovering forgeries.

---

<sup>1</sup>A Lambertian surface for reflection is a surface that appears uniformly bright from all directions of view and reflects the entire incident light. Lambertian reflectance is the property exhibited by an ideal matte or diffusely reflecting surface.



Figure 1.5: Original image (left) and the extracted shadows constraints (right)

Based on this model, the authors proposed to construct two geometric constraints: the first one is based on the relationship of connecting lines. A connecting line is a line that connects some object point with its shadow. According to planar homology, all of these connecting lines intersect in a vanishing point.

The second constraint is based on the ratio of these connecting lines. In addition, the authors also proposed to explore the changing ratio along the normal direction of the shadow boundaries.

Geometric and shadow photometric constraints together are used to detect image compositions. However, in spite of being a good initial step in forensic shadow analysis, the major drawback of the method is that it only works with images containing casting shadows, a very restricted scenario.

### 1.4.3 *Inconsistencies in light color*

The last group of methods investigate the presence, or not, of composition operations in digital images using color inconsistencies.

Gholap and Bora [9] [7] pioneered this approach using the *illuminant colors*. For that, the authors used a *dichromatic reflection model* proposed by Tominaga and Wandell [15], which assumes a single light source to estimate illuminant colors from images.

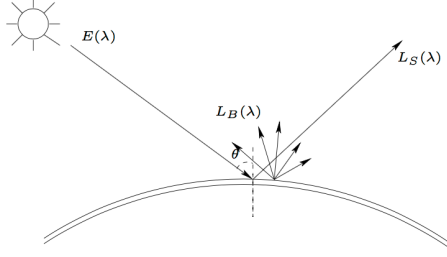


Figure 1.6: The dichromatic reflection model

According to this model, reflection of any non-homogeneous materials may be modelled as additive mixture of two components, diffused reflection and surface reflection as shown in Fig. ??.

Considering an object point illuminated by a light source, the reflected ray consists of diffuse reflection  $L_B(\lambda)$  and surface reflection  $L_S(\lambda)$ . The reflected light  $L(\Theta, \lambda)$  can be written as:

$$L(\Theta, \lambda) = m_S(\Theta)L_S(\lambda) + m_B(\Theta)L_B(\lambda) \quad (1.1)$$

where  $m_S(\Theta)$  and  $m_B(\Theta)$  are geometrical factors and  $\Theta$  the angle of the incident light. This equation can be rewritten in terms of RGB sensors in matrix form.

The two vectors  $L_B(\lambda)$  and  $L_S(\lambda)$  span the two dimensional plane called *dichromatic plane*.

Dichromatic planes can also be estimated using principal component analysis (PCA) from each specular highlight region of an image. By applying a *Singular Value Decomposition (SVD)* on the RGB matrix extracted from highlighted regions, the authors extract the eigenvectors associated with the two most significant eigenvalues to construct the *dichromatic plane*. This plane is then mapped onto a straight line, named dichromatic line, in normalized *r-g-chromaticity* space.

For distinct objects illuminated by the same light source, the intersection point produced by their dichromatic line intersection represents the illuminant color. If the image has more than one illuminant, it will present more than one intersection point, which is not expected to happen in pristine (non-forged images). This method represented the first important step toward forgery de-

tection using illuminant colors, but has some limitations such as the need of well defined specular highlight regions for estimating the illuminants.

Following Gholap and Bora’s work, Riess and Angelopoulou [12] used an extension of the *Inverse-Intensity Chromaticity Space*, originally proposed by Tan et al. [14], to estimate illuminants locally from different parts of an image for detecting forgeries.

In addition, Wu and Fang [17] proposed a new way to detect forgeries using illuminant colors. Their method divides a color image into overlapping blocks estimating the illuminant color for each block. To estimate the illuminant color, the authors proposed to use the algorithms Gray-World, Gray-Shadow and Gray-Edge [16].

These approaches will be better explained in the next section due their importance for this proposed method.

## 1.5 Illuminant color estimation

The color of an object observed in an image depends both on its intrinsic color and the color of light source i.e., the illuminant.

It is important to keep in mind that even the same light source can generate different illuminants. The illuminant formed by the sun, for example, varies in its appearance during the day and time of year as well as with the weather. We only capture the same illuminant, measuring the sunlight at the same place at the same time.

We can explore illuminants in forensics to check the consistency of similar objects in a scene. If two objects with very similar color stimuli (e.g., human skin) depict inconsistent appearance (different illuminants), it means they might have undergone different illumination conditions hinting at a possible image composition. On the other hand, if we have a photograph with two people and the color appearance on the faces of such people are consistent, it is likely they





Figure 1.7: An example of a generated distance map using Riess and Angelopoulou [12] approach. From left to right: (a) the original image, (b) *illuminant map*, (c) generated distance map

have undergone similar lighting conditions.

Riess and Angelopoulou [12] pioneered the approach of using a color-based method that investigates illuminant colors to detect forgeries in forensic scenario. In their work illuminant colors are estimated locally, effectively decomposing the scene in a map of differently illuminated regions. Inconsistencies in such a map suggest possible image tampering.

The method can be divided into four steps:

1. Image segmentation. The image is segmented into regions, called *superpixels*, of approximately the same object color. Each superpixel follows must be:
  - (a) Directly illuminated by the same light source.
  - (b) Compliant with the *dichromatic reflectance model* [14].
2. Manual user selection of superpixels under investigation.
3. Local illuminant color estimation for each superpixel (both for segmented superpixels and user selected regions).
4. Reference illuminant selection (manual) and *distance map* evaluation. The distance map is the base for an expert analysis for forgery detection.

The final decision of this approach is delegated to an expert and not to the algorithm itself.

### 1.5.1 Illuminant maps

#### 1.5.1.1 Generalized Greyworld estimation

The starting point is the *gray world assumption*, proposed by Buchsbaum [1]. In its simplest version, it is assumed that information in the average of each channel of the image is the representative gray level.

Let  $f(x) = (\Gamma_R(x), \Gamma_G(x), \Gamma_B(x))^T$  the RGB color of a pixel at position  $x$  and  $\Gamma_i(x)$  the intensity of that pixel in the  $i$ -th channel. In their paper, Van de Weijer et al. assumes that the diffuse reflection is diffuse and that the camera response is linear. It is also assumed that the scene is illuminated by a single light source.

The RGB color  $f(x)$  can also be rewritten as

$$f(x) = \int_{\omega} e(\beta, x) s(\beta, x) c(\beta) d\beta \quad (1.2)$$

where  $\omega$  is the visible light spectrum,  $\beta$  is the light wavelength,  $e(\beta, x)$  is the illuminant spectrum,  $s(\beta, x)$  is the surface reflectance of an object and  $c(\beta)$  is the color sensitivities of the camera for each channel.

As an alternative to the gray-world hypothesis, Van de Weijer et al. [16] proposed the *gray-edge hypothesis*: the average of the reflectance differences in a scene is achromatic.

This idea led to a framework for low-level based illuminant estimation, called *Generalized Grayworld*.

$$\left( \int \left| \frac{\delta^n f^\sigma(x)}{\delta x^n} \right|^p dx \right)^{\frac{1}{p}} = k e^{n,p,\sigma} \quad (1.3)$$

where  $k$  denotes a scaling factor,  $|\cdot|$  the norm operand,  $\delta$  the differential operator and  $f^\sigma(x)$  the pixel intensities at position  $x$ , smoothed with a Gaussian kernel  $\sigma$ .

This framework 1.3 produces different estimations for the illuminant color

based on three parameters:

1. The order  $n$  determines if the method is a gray-world or a gray-edge algorithm. The gray-world methods are based on the RGB values, whereas the gray-edge methods are based on the spatial derivative of order  $n$ .
2. The Minkowski norm  $p$  which determines the relative weights of the multiple measurements from which the final illuminant color is estimated.
3. The scale  $\sigma$  of the local measurements. For first or higher order estimation, this local scale is combined with the differentiation operation computed with the Gaussian derivative. For zero-order gray-world methods, this local scale is imposed by a Gaussian smoothing operation.

On varying of these parameter, a different method can be used. An overview of the possible methods derived from Eq. 1.3 is displayed in Table 1.1.

#### 1.5.1.2 Inverse Intensity-Chromaticity estimation

The other considered illuminant estimation method is based on the idea proposed by Tan et al. [14], called *inverse intensity-chromaticity*.

The base for these kind of approach is the dichromatic reflectance model [9], which states that the amount of light reflected from a point,  $x$ , of a dielectric, non-uniform material is a linear combination of diffuse reflection and specular reflection. Further assumptions are that the color of the specularities approximates the color of the illuminant, and that the camera response is linear.

Considering a trichromatic camera, the sensor response  $I_c(x)$ , for each color channel  $c \in \{R, G, B\}$  is:

$$I_c(x) = m_S(x)L_S(x) + m_B(x)L_B(x) \quad (1.4)$$

as described in 1.1.

Table 1.1: Overview of different illuminant estimation methods based on 1.3

Name	Symbol	Equation	Assumption
Gray-World	$e^{0,1,0}$	$(\int f(x)dx) = ke$	The average reflectance in a scene is achromatic
max-RGB	$e^{0,\infty,0}$	$(\int  f(x) ^\infty dx)^{\frac{1}{\infty}} = ke$	The maximum reflectance in a scene is achromatic
Shades of Gray	$e^{0,p,0}$	$(\int  f(x) ^p dx)^{\frac{1}{p}} = ke$	The $p$ -th Minkowski norm of scene is achromatic
General Gray-World	$e^{0,p,\sigma}$	$(\int  f^\sigma(x) ^p dx)^{\frac{1}{p}} = ke$	The $p$ -th Minkowski norm of scene is achromatic after smoothing
Gray-Edge	$e^{1,p,\sigma}$	$(\int  f_x^\sigma(x) ^p dx)^{\frac{1}{p}} = ke$	The $p$ -th Minkowski norm of the image derivative is achromatic
Max-Edge	$e^{1,\infty,\sigma}$	$(\int  f_x^\sigma(x) ^\infty dx)^{\frac{1}{\infty}} = ke$	The maximum reflectance difference in a scene is achromatic
2nd order Gray-Edge	$e^{2,p,\sigma}$	$(\int  f_{xx}^\sigma(x) ^p dx)^{\frac{1}{p}} = ke$	The $p$ -th Minkowski norm of the second order derivative in a scene is achromatic

Let  $\sigma_c$  the image chromaticity,  $\Delta_c(x)$  the diffuse chromaticity and  $\Gamma_c(x)$  the specular chromaticity defined as follows:

$$\sigma_c(x) = \frac{I_c(x)}{\sum_i I_i(x)} \text{ where } i \in \{R, G, B\} \quad (1.5)$$

$$\Delta_c(x) = \frac{L_{S,c}(x)}{\sum_i L_{S,i}(x)} \text{ where } i \in \{R, G, B\} \quad (1.6)$$

$$\Gamma_c(x) = \frac{L_{B,c}(x)}{\sum_i L_{B,i}(x)} \text{ where } i \in \{R, G, B\} \quad (1.7)$$

Thus the Eq. 1.4 can be rewritten as

$$I_c(x) = m_S(x)\Delta_c(x) + m_B(x)\Gamma_c(x) \quad (1.8)$$

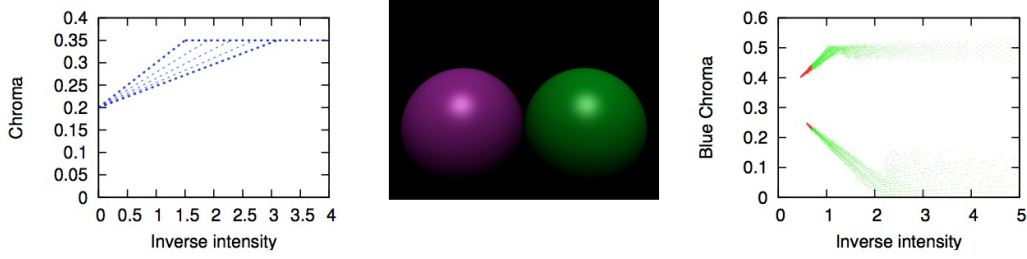


Figure 1.8: Pixel distribution in inverse-intensity chromaticity (IIC) space. Left are as ideal distribution, left on a synthetic image (in the center).

Tan et al. [14] derived a linear relationship between diffuse, specular and image chromaticities:

$$\sigma_c(x) = m(x) \frac{1}{\sum_i I_i(x)} + \Gamma_c(x) \quad (1.9)$$

where  $i \in \{R, G, B\}$  and  $m(x)$  is a geometrical factor (light position, surface orientation, camera position, ...), that can be approximated. In the illuminant estimation, the most important aspect is the  $y$ -intercept  $\Gamma_c$ .

The 2D space defined by  $\frac{1}{\sum_i I_i(x)}$  as domain and  $0 \leq \sigma_c \leq 1$  as range is called *inverse-intensity chromaticity (IIC)* space.

An example of the IIC plots for a single channel of a synthetic image are shown in Fig. 1.8. Pixels from the green and purple balls form two clusters. The clusters have spikes that point towards the same location at the  $y$ -axis. Considering only such spikes from each cluster, the illuminant chromaticity is estimated from the joint  $y$ -axis intercept of all spikes in IIC space.

Instead of examining the entire pixel distribution, Riess et al. [12] perform the analysis over small connected image regions of roughly uniform object color (*superpixels*). Depending on the outcome of our shape analysis, we can either use this local region to obtain an illuminant estimate, or reject it if it does not seem to fulfill the underlying assumptions of the proposed model. Using local regions allows us to incorporate multiple sampling and voting in the estimation of local illuminants.

## 1.6 Human faces splicing detection

The approach proposed in Chapter 2 is based on two different works, published by Carvalho et al. [2] and Fan et al. [3].

The method proposed by Carvalho et al. [2] aims to detect splicing focusing on human faces, minimizing the user interaction. Faces are previously labeled by a human selecting the box within is contained, than the process will associate a label to each face (i.e. *normal* or *fake*).

The method can be divided into four steps:

1. *Description*: in this step illuminant maps are estimated with the two different approaches, GGE and IIC, and feature vector are generated. Each feature vector is associated with a face pair.

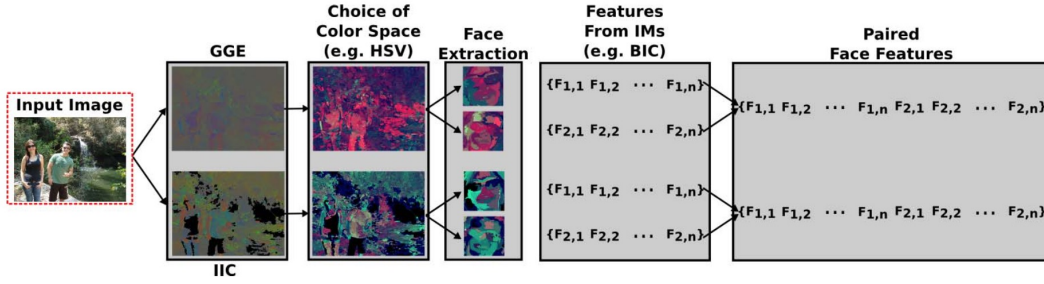


Figure 1.9: Image description pipeline for extracting paired face feature vectors

The Fig. 1.9 shows the image description extraction pipeline. Given an input image, the illuminant maps are estimated and converted to a selected color space (e.g. HSV). So, the faces in the image are extracted (using the defined area). For each face a descriptor is used to generate a feature vector (e.g a color descriptor, texture descriptor or shape descriptors) and finally they are coupled in order to generate paired feature vector simply concatenating the two original vectors.

In this step multiple descriptors and color spaces are used in order to increment the number of final classifiers.

2. *Face Pair Classification*: a set of classification models are trained using the previous step feature vectors. Based on the number of color spaces and descriptors used, a set of KNN classifiers are trained over the paired face feature vectors. The final result is given by a majority voting of all the selected classifiers.
3. *Forgery Classification*: given an image  $I$  containing  $q$  people (faces), it is characterized by a set  $\mathcal{S} = \{\mathcal{P}_1, \dots, \mathcal{P}_m\}$ , where  $\mathcal{P}_i$  is the  $i$ -th paired feature vector and  $m = \frac{q(q-1)}{2}, q \geq 2$ . If any  $\mathcal{P}_i \in \mathcal{S}$  is classified as fake, the image  $I$  is classified as fake. Otherwise, the image is considered as pristine.
4. *Forgery Detection*: once knowing that an image is fake, in this stage it is identified which one is more likely to be fake in the image. This is done using a specific SVM classifier.

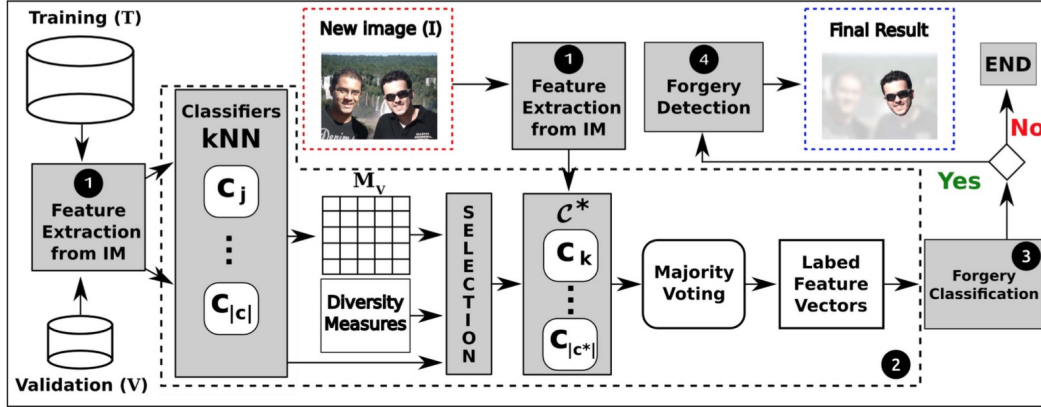


Figure 1.10: Image splicing detection over human faces

The Fig. 1.10 shows the above described method pipeline.

### 1.6.1 Method drawbacks

The main drawback of this approach relies in the manual selection of faces by a human agent. The definition of a face in the image by the operator is made

by identification of the bounding box in which it is fully contained.

This manual operation does not allow a blind approach to the problem. Because the faces are considered in pairs, this method can be applied only in the case when there are at least two faces, so you need to know in advance the content of the images to assess the applicability of this algorithm.

Working with pairs of faces, another problem is the choice of which face has been manipulated among those considered.

In addition, this method is based on the observation that, given two faces (a pristine face and a spliced one), the difference between the two forged faces illuminant maps tend to be higher. This intuition, however, proved to be not applicable in all contexts, so cannot be considered as a starting point for the final evaluation.

## 1.7 Region splicing detection

The other considered approach is based on the work of Fan et al. [3]. This method relies on the Van de Weijer et al. [16] Generalized Gray-World framework 1.3. These algorithm perform better on a scene when it is rich of colors, but in a splicing detection scenario we are interest in a specific region of the image.

This approach splits image in vertical and horizontal bands (rectangular regions), assuming that each band contains sufficient colors for a correct illuminant estimation. Five different algorithm are used, deduced from Eq. 1.3: Grey-World, Max-RGB, Shades of Grey, first- order Grey-Edge and second-order Grey-Edge, in order to have as many illuminant estimates for each band.

This algorithm can be divided into two steps:

1. Subsampling of the image horizontally and vertically
2. Illuminant estimation for each band using the 5 different algorithms and spliced region location.



In the first step the image is sampled into two band categories: horizontal and vertical bands. The height and the width of each band is configured *a priori* based on the minimal height and minimal width separately among the objects of interest. An object of interest is encompassed by a virtual rectangle with its height and width decided by the object itself.

The second step can be also divided into five steps:

1. For each direction and for each algorithm, a reference illuminant is estimated for a single band.
2. For each direction and for each algorithm, a reference illuminant for each direction is evaluated as the median of all references of that direction. At this stage there are two reference illuminants (one for the vertical and one for the horizontal direction) for each algorithm.
3. A detection map is created, with the same dimensions of the image.
4. For each algorithm, every band estimate are compared with the reference illuminant of that band direction and algorithm with the Euclidean distance. If the distance exceed a fixed threshold, the band is considered fake and all the pixel values in the detection map are increased by one unit.
5. The forgery is located using the resulting thresholded detection map.

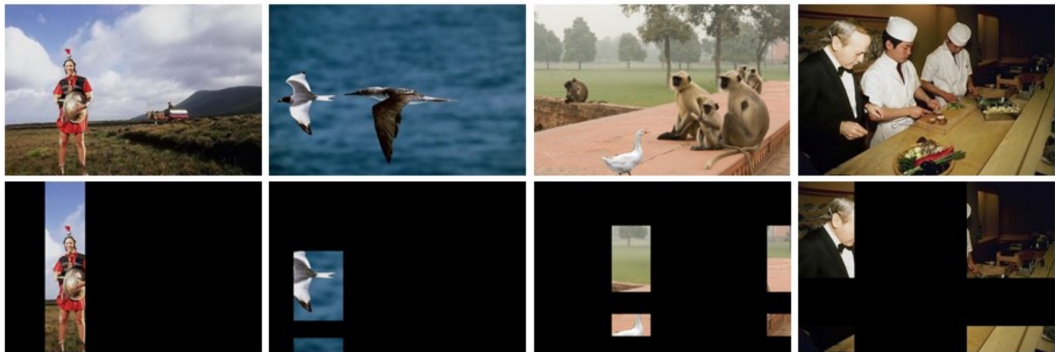


Figure 1.11: Image regions splicing detection

The main advantage of this method is its blind approach: the algorithm is not based on the image content (as it was in the previous case) and no human interaction is needed. The only parameters are the bands minimal dimensions and the threshold. Due these facts it is very simple to implement, but it is also afflicted by false alarm caused by a not easy to tune threshold (which is the key the final step).

### ***1.7.1 Method drawbacks***

Given its simplicity, this approach has some drawbacks. First, because the classification is based on a simple distance between a reference value, a key point is the identification of optimal thresholds.

These thresholds can be calculated experimentally, but their accuracy will depend on the dataset with which they were computed.

For how it's built, moreover, this method tends to have a low detection rate compared to a high false positive rate.

# Chapter 2

## Proposed approach

In the previous chapter, a review of two splicing detection methods based on illuminant colors analysis has been presented. However, their effectiveness still needed to be improved for real forensic applications.

The approach proposed in this chapter has been developed to correct some drawbacks and mainly to achieve an improved accuracy over the two approaches presented in Chapter 1.

### 2.1 Overview

Most of the times, the splicing detection process relies on the expert's experience and background knowledge. This process usually is time consuming and error prone once that image splicing is more and more sophisticated and an aural (e.g., visual) analysis may not be enough to detect forgeries.

This approach to detecting image splicing is developed aiming at minimizing the user interaction.

The two methods, presented in the previous chapter [2] and [3], are now being used in synergy with each other, going to analyze each image at the same time looking for potential signs of forgery.

Starting from an image we want to analyze, the method will output a set of results.

- A classification **label** indicating whether an image is believed to be original

or counterfeit.

- A classification **score** indicating the confidence of the method output.
- A **detection map** highlighting the detected spliced regions.

The proposed approach minimizes human interaction being fully automated. However, not both the modules can operate in any circumstance. The face splicing detection module will work only if there is a number of faces greater than or equal to two.

## 2.2 Face splicing detection module

## 2.3 Region splicing detection module

The second form of the algorithm is to implement the method proposed by Fan et al. [3] with some changes in order to try to correct some of its major drawbacks presented in Section 1.7.

The splicing detection task performed by our approach consists in labelling a new image among two pre-defined classes (real and fake) and later pointing the face with higher probability to be the fake face. In this process, a classification model is created to indicate the class to which a new image belongs.

In summary, this module consists of the 6 main steps:

- **Image segmentation:** relies on vertical and horizontal image segmentations. The outputs of this stage are two set of directional image bands.
- **Band illuminant estimation:** consists in estimating the illuminant color for each segmented band using 5 different GGE algorithms.
- **Reference illuminant estimation:** consists in estimating the illuminant reference value for each direction.

- **Feature vector evaluation:** relies on encoding the singular band illuminant information into a feature vector for further classification. The feature vector elements are the differences between the current illuminant color and the reference one.
- **Band classification:** consists in labelling each image band into one of the know classes (real or fake) based on the previously learned classification model.
- **Detection map:** using the classification output of the previous step, a detection map is build. The higher the value of this map, the higher the resulting classification score for a single pixel.

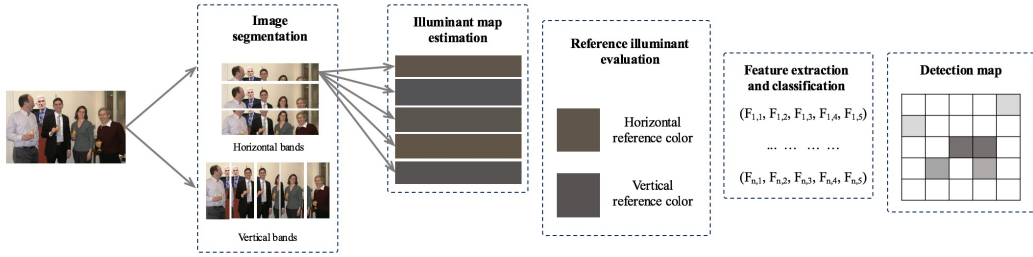


Figure 2.1: Image regional splicing detection module pipeline

The Fig 2.1 summarize the module pipeline.

### 2.3.1 Image segmentation

In the first step of the process, the input image is segmented in order to obtain two image bands categories: horizontal and vertical bands. This kind of segmentation method is chosen because of its simplicity.

First, a band width  $B_w$  and a band height  $B_h$  is set. Due to the fact that the segmentation has to produce overlapping bands, we set a delta factor of  $\frac{1}{4}$ . As a result we get overlapping stripes for a total of 25% of their area.

The choice of the band size is a crucial phase of the algorithm: a band too tight would fail to capture the information necessary to classify our object of interest as falsified, unlike a band too wide would capture instead too much additional information.

The choice of the overlapped area percentage makes possible a more detailed evaluation. In this way it is possible to classify the same region of the image more than once, increasing the expressive power of our final classifier, the detection map.

In summary, let  $I$  be the input image. After the segmentation process we obtain a set  $B$  of bands containing all vertical and horizontal bands:

$$B = \{V_1, \dots, V_n, H_1, \dots, H_m\}$$

The dimension of  $B$  is given by the sum of the number of vertical ( $n$ ) and horizontal ( $m$ ) bands.

### 2.3.2 *Band illuminant estimation*

The resulting image bands are now processed in order to evaluate the illuminant color using different techniques.

For this step, the Generalized Grayworld [16] algorithms are used, as presented in Chapter 1. For each band, the illumination estimation is accomplished by using one of algorithms composed of Grey-World, Max-RGB, Shades of Grey, first-order Grey-Edge and second-order Grey-Edge. Thus we have 5 illuminant estimates for each band. Table 1.1 in Chapter 1 summarize this algorithm parameters.

In this way we obtain 5 different illuminant estimation for each single band.

$$\forall b \in B \quad R_a(b) = GGE_a(b) \quad a \in \mathcal{A}$$

where  $\mathcal{A}$  is the set of the previously mentioned algorithms and  $GGE$  is the

algorithm implementation.

### *2.3.3 Reference illuminant estimation*

### *2.3.4 Feature vector estimation*

### *2.3.5 Band classification*

### *2.3.6 Detection map*

# Chapter 3

## Experiments and results

### 3.1 Evaluation datasets

#### 3.1.1 *Colorchecker*

The ColorChecker dataset is a collection of images for evaluating Color Constancy algorithms built as additional material to [8]. It consists in 568 RGB colored images of different scenes, both indoor and outdoor taken under different illuminations. In each scene a Gretag MacBeth Color Checker Chart was placed such that it was illuminated by the main scene illuminant and thus its color could be retrieved. The data is available in Canon RAW format free of any correction.



Figure 3.1: Example of an image of the ColorChecker dataset

This dataset has been mainly used for experimenting on pristine data: due



its characteristics is very varied and lends itself well to image analysis based on color.

### 3.1.2 *DSO-1*

The DSO-1 dataset<sup>1</sup> is composed of 200 indoor and outdoor images with image resolution of  $2048 \times 1536$  pixels. Out of this set of images, 100 are original, i. e., have no adjustments whatsoever, and 100 are forged.



Figure 3.2: Example of an image of the DSO-1 dataset

The forgeries were created by adding one or more individuals in a source image that already contained one or more people. When necessary, we complemented an image splicing operation with post-processing operations (such as color and brightness adjustments) in order to increase photorealism.

### 3.1.3 *DSI-1*

The DSI-1 dataset is composed of 50 images (25 original and 25 doctored) downloaded from different websites in the Internet with different resolutions. Original

---

<sup>1</sup>Public available for download at <https://recodbr.wordpress.com/code-n-data>

images were downloaded from Flickr and doctored images were collected from different websites such as Worth 1000, Benetton Group 2011, Planet Hiltron, etc.



Figure 3.3: Example of an image of the DSI-1 dataset

#### 3.1.4 *NIMBLE*

### 3.2 Test cases

### 3.3 Performance

# Conclusions

# Bibliography

- [1] G. Buchsbaum. A spatial processor model for object colour perception. *Journal of the Franklin Institute*, 310(1):1 – 26, 1980.
- [2] T. Carvalho, F. A. Faria, H. Pedrini, R. d. S. Torres, and A. Rocha. Illuminant-based transformed spaces for image forensics. *IEEE Transactions on Information Forensics and Security*, 11(4):720–733, 2016.
- [3] Y. Fan, P. Carré, and C. Fernandez-Maloigne. Image splicing detection with local illumination estimation. In *Image Processing (ICIP), 2015 IEEE International Conference on*, pages 2940–2944. IEEE, 2015.
- [4] H. Farid. Digital doctoring: can we trust photographs? 2009.
- [5] H. Farid. Image forgery detection. *IEEE Signal processing magazine*, 26(2):16–25, 2009.
- [6] G. D. Finlayson and E. Trezzi. Shades of gray and colour constancy. In *Color and Imaging Conference*, volume 2004, pages 37–41. Society for Imaging Science and Technology, 2004.
- [7] K. Francis, S. Gholap, and P. Bora. Illuminant colour based image forensics using mismatch in human skin highlights. In *Communications (NCC), 2014 Twentieth National Conference on*, pages 1–6. IEEE, 2014.
- [8] P. V. Gehler, C. Rother, A. Blake, T. Minka, and T. Sharp. Bayesian color constancy revisited. In *Computer Vision and Pattern Recognition, 2008. CVPR 2008. IEEE Conference on*, pages 1–8. IEEE, 2008.
- [9] S. Gholap and P. Bora. Illuminant colour based image forensics. In *TENCON 2008-2008 IEEE Region 10 Conference*, pages 1–5. IEEE, 2008.

- [10] M. K. Johnson and H. Farid. Exposing digital forgeries by detecting inconsistencies in lighting. In *Proceedings of the 7th Workshop on Multimedia and Security, MM&#38;Sec '05*, pages 1–10, New York, NY, USA, 2005. ACM.
- [11] B. Mazin, J. Delon, and Y. Gousseau. Estimation of illuminants from projections on the planckian locus. *IEEE Transactions on Image Processing*, 24(6):1944–1955, 2015.
- [12] C. Riess and E. Angelopoulou. Scene illumination as an indicator of image manipulation. In *International Workshop on Information Hiding*, pages 66–80. Springer, 2010.
- [13] C. Springer. Geometry and analysis of projective spacesfreeman. *New York*, 1964.
- [14] R. T. Tan, K. Nishino, and K. Ikeuchi. Color constancy through inverse-intensity chromaticity space. *JOSA A*, 21(3):321–334, 2004.
- [15] S. Tominaga and B. A. Wandell. Standard surface-reflectance model and illuminant estimation. *JOSA A*, 6(4):576–584, 1989.
- [16] J. Van De Weijer, T. Gevers, and A. Gijsenij. Edge-based color constancy. *IEEE Transactions on image processing*, 16(9):2207–2214, 2007.
- [17] X. Wu and Z. Fang. Image splicing detection using illuminant color inconsistency. In *Multimedia Information Networking and Security (MINES), 2011 Third International Conference on*, pages 600–603. IEEE, 2011.
- [18] W. Zhang, X. Cao, J. Zhang, J. Zhu, and P. Wang. Detecting photographic composites using shadows. In *Multimedia and Expo, 2009. ICME 2009. IEEE International Conference on*, pages 1042–1045. IEEE, 2009.
- [19] B. B. Zhu, M. D. Swanson, and A. H. Tewfik. When seeing isn’t believing [multimedia authentication technologies]. *IEEE Signal Processing Magazine*, 21(2):40–49, 2004.

# Ringraziamenti